New Phytologist

Research

Singlet oxygen production by photosystem II is caused by misses of the oxygen evolving complex

Heta Mattila, Sujata Mishra, Taina Tyystjärvi and Esa Tyystjärvi

Department of Life Technologies/Molecular Plant Biology, University of Turku, FI-20014 Turku, Finland

Author for correspondence:
Esa Tyystjärvi
Email: esatyy@utu.fi

Received: *2 May 2022*
Accepted: *10 September 2022*

New Phytologist (2022)
doi: 10.1111/nph.18514

Key words: anaerobic, anoxia, cyanobacteria, F_V/F_M, histidine, photodamage, reactive oxygen species.

Summary

- Singlet oxygen ($^1O_2$) is a harmful species that functions also as a signaling molecule. In chloroplasts, $^1O_2$ is produced via charge recombination reactions in photosystem II, but which recombination pathway(s) produce triplet Chl and $^1O_2$ remains open. Furthermore, the role of $^1O_2$ in photoinhibition is not clear.
- We compared temperature dependences of $^1O_2$ production, photoinhibition, and recombination pathways.
- $^1O_2$ production by pumpkin thylakoids increased from −2 to +35°C, ruling out recombination of the primary charge pair as a main contributor. $S_2Q_A^-$ or $S_2Q_B^-$ recombination pathways, in turn, had too steep temperature dependences. Instead, the temperature dependence of $^1O_2$ production matched that of misses (failures of the oxygen (O_2) evolving complex to advance an S-state). Photoinhibition *in vitro* and *in vivo* (also in *Synechocystis*), and in the presence or absence of O_2, had the same temperature dependence, but ultraviolet (UV)-radiation-caused photoinhibition showed a weaker temperature response.
- We suggest that the miss-associated recombination of $P_{680}^+Q_A^-$ is the main producer of $^1O_2$. Our results indicate three parallel photoinhibition mechanisms. The manganese mechanism dominates in UV radiation but also functions in white light. Mechanisms that depend on light absorption by Chls, having $^1O_2$ or long-lived P_{680}^+ as damaging agents, dominate in red light.

Introduction

Molecular oxygen (O_2) in its ground state is a biradical, as the two unpaired electrons have parallel spins (thus, O_2 is a triplet). Exchange of energy and spin with a molecule in a triplet excited state can turn O_2 to a highly reactive singlet state ($^1O_2$) – for a review, see Schweitzer & Schmidt (2003). $^1O_2$ causes cellular damage by oxidizing biomolecules containing double bonds (Schweitzer & Schmidt, 2003; Halliwell & Gutteridge, 2015; Di Mascio *et al.*, 2019). $^1O_2$ also generates cellular signals leading to acclimation to high light and/or to cell death via apoptotic pathways in photosynthetic organisms (Lee *et al.*, 2007; Ramel *et al.*, 2012b; Crawford *et al.*, 2018).

Both photosystem I (PSI) and photosystem II (PSII) produce $^1O_2$ (Macpherson *et al.*, 1993; Cazzaniga *et al.*, 2012), the majority being produced by the PSII core after a charge recombination reaction (Telfer *et al.*, 1994; Ramel *et al.*, 2012a); however, contrasting data have also been published (Santabarbara *et al.*, 2007). The excited triplet state of the PSII reaction center Chl(s) ($^3P_{680}$) can react with the ground-state O_2, which results in the formation of $^1O_2$ and the singlet ground state of P_{680}. $^3P_{680}$ can be produced by the recombination of the charge pairs $S_2Q_A^-$, $S_3Q_A^-$, $S_2Q_B^-$, and $S_3Q_B^-$, by the recombination of the primary charge pair $P_{680}^+Pheo^-$, or by the recombination of $P_{680}^+Q_A^-$. The recombination reactions $S_{2/3}Q_{A/B}^- \rightarrow S_{1/2}Q_{A/B}$ are rare, with time constant of *c.* 1 s for $S_2Q_A^-$ and 20–30 s for $S_2Q_B^-$ (Rutherford, 1989; Tyystjärvi & Vass, 2004), but have been suggested to be responsible for $^1O_2$ production in weak light (Keren *et al.*, 1997). The primary pair, in turn, recombines with nanosecond kinetics and may produce $^3P_{680}$ when Q_A is reduced (Vass & Styring, 1993). The $P_{680}^+Q_A^-$ pair is available for recombination only if the O_2-evolving complex (OEC) of PSII fails to reduce P_{680}^+.

A transient failure of the OEC to reduce P_{680}^+ is called a miss, and *c.* 8% of charge separations fail in this way (Forbush *et al.*, 1971; Isgandarova *et al.*, 2003; Pham *et al.*, 2019). In this case, charge separation leads to reduction of Q_A, followed by recombination of $P_{680}^+Q_A^-$. Misses represent reaction equilibria between S-state advancement and recombination reaction in normal, active PSII. The percentage of misses is similar in the thermophilic cyanobacterium *Cyanosiphon merolae* and in spinach, although the redox potential of the Q_A/Q_A^- pair is much less negative in *C. merolae* than in spinach (Pham *et al.*, 2019). Furthermore, the time constant of the recombination of $P_{680}^+Q_A^-$ is 100–200 μs in Tris-washed thylakoids, which lack a functional donor side (Renger & Wolff, 1976); the kinetics in active PSII are not known. A 100–200 μs time constant of the $P_{680}^+Q_A^-$ recombination reaction would make misses highly competitive

against the majority of S-state transitions. These considerations imply that a miss occurs because the rate of S-state advancement in a fraction of OECs is so slow that $P_{680}{}^{+}Q_A{}^{-}$ recombines, not because the recombination occasionally wins competition with normal advancement of the S-state. Electron paramagnetic resonance (EPR) measurements (Han *et al.*, 2012) and modeling of flash O_2 data (Pham *et al.*, 2019) indicate that most misses occur in the S_2 to S_3 transitions, but other S-states may also fail to advance.

It has been suggested that $^1O_2$ is responsible for photoinhibition of PSII – for reviews, see Vass (2012), Tyystjärvi (2013), and Zavafer & Mancilla (2021) – as positive shifts in the redox potentials of PSII electron acceptors limit $^1O_2$ production and protect against photoinhibition (Fufezan *et al.*, 2002, 2007; Davis *et al.*, 2016; Treves *et al.*, 2016) and because PSII can be protected by carotenoids that quench $^1O_2$ (Jahns *et al.*, 2000; Hakkila *et al.*, 2013). However, photoinhibition is known to occur under ultraviolet (UV) radiation (Jones & Kok, 1966; Hakala *et al.*, 2005) and in anaerobic conditions (Nedbal *et al.*, 1992; Sundby *et al.*, 1992) where $^1O_2$ is not formed (Hideg *et al.*, 1994), indicating that either $^1O_2$ does not cause photoinhibition or photoinhibition has alternative or parallel mechanisms. In addition, $^1O_2$ is known to slow down the PSII repair cycle, as it damages oxidation-prone translation factors, reducing the overall translation efficiency (Nishiyama *et al.*, 2004).

To better understand $^1O_2$ production and photoinhibition, we measured their temperature dependences and compared them with temperature dependences of recombination pathways. The results indicate that the miss-associated recombination reaction is crucial for the formation of $^1O_2$. The temperature dependence of photoinhibition, in turn, was similar but not identical under different wavelengths, suggesting that several mechanisms contribute to photoinhibition. In white light, the contribution of the manganese (Mn) mechanism (Hakala *et al.*, 2005) was estimated to be 63–68%. Under monochromatic light, contributions from two other mechanisms (a $^1O_2$-dependent and a $P_{680}{}^{+}$-dependent mechanism) increase toward longer wavelengths.

Materials and Methods

Growth conditions

Pumpkin (*Cucurbita maxima* L.) was grown at 20°C, in a 16 h light period, with photosynthetic photon flux density (PPFD) 150–200 μmol m^{-2} s^{-1}. Thylakoid membranes were isolated as previously described (Hakala *et al.*, 2005) and stored at −75°C in a storage buffer (10 mM HEPES (pH 7.4), 0.5 M sorbitol, 10 mM magnesium chloride ($MgCl_2$), and 5 mM sodium chloride (NaCl)). *Synechocystis* sp. PCC 6803 cells were maintained on BG-11 agar plates (Rippka *et al.*, 1979) supplied with 20 mM HEPES–sodium hydroxide (NaOH) (pH 7.5), under continuous light (PPFD 40 μmol m^{-2} s^{-1}) at 32°C. A few days before the experiments, *Synechocystis* cells were transferred to liquid cultures with mixing, otherwise under similar conditions.

Singlet oxygen measurements

Pumpkin thylakoids (100 μg Chl ml^{-1}) were incubated for 5 min in a photoinhibition buffer (40 mM HEPES–potassium hydroxide (pH 7.4), 1 M betaine monohydrate, 330 mM sorbitol, 5 mM $MgCl_2$, and 5 mM NaCl) in darkness and then illuminated for 2 min with strong light, and the light-induced changes in O_2 concentration in the absence and presence of 20 mM L-histidine (Sigma-Aldrich) were recorded (Telfer *et al.*, 1994; Rehman *et al.*, 2013). An optode (Firesting O_2 FSO2-0x with OXSP5 sensor spots; PyroScience GmbH, Aachen, Germany), a homemade cuvette, and a 10 W cold-white LED (PPFD 2000 μmol m^{-2} s^{-1}; for the spectrum, see Supporting Information Fig. S1) were used for measurements at 5, 15, 25, and 35°C. The optode was calibrated with air-saturated water. A measurement at −2°C, where water cannot be used for calibration, and a comparison measurement at 15°C, were done using an O_2 electrode (Hansatech, King's Lynn, UK) and a slide projector equipped with a halogen lamp (PPFD 3000 μmol m^{-2} s^{-1}; for the spectrum, see Fig. S1). The O_2 electrode was calibrated with air-saturated photoinhibition buffer that remained liquid at −2°C, before and after addition of solid sodium dithionite to remove O_2. With both devices, the rate of $^1O_2$ production was calculated as the difference in the rate of O_2 consumption in the presence and absence of 20 mM histidine. The temperature dependence of the reaction between histidine and $^1O_2$ was tested by illuminating (PPFD 2000 μmol m^{-2} s^{-1}) 1 μM rose bengal in the presence of 20 mM histidine. No significant consumption of O_2 was observed in the absence of histidine.

Recombination reactions

Thermoluminescence was measured with a homemade luminometer from pumpkin thylakoids (600 μg Chl ml^{-1}) as previously described (Tyystjärvi *et al.*, 2009), in the presence and absence of 20 μM 3-(3,4-dichlorophenyl)-1,1-dimethylurea (DCMU), with a heating rate of 0.56°C s^{-1}. A 1 J xenon pulse was fired at −10°C. The rate constants of the $S_{2/3}Q_{A/B}{}^{-}$ recombination reactions were calculated as functions of temperature with COPASI (Hoops *et al.*, 2006) assuming that each rate constant depends on temperature according to the Arrhenius equation. Three competing recombination routes (direct, indirect, and excitonic) were assumed for the analysis of the Q band (Rappaport & Lavergne, 2009), whereas the B band was analyzed as a single reaction (Randall & Wilkins, 1945; Tyystjärvi & Vass, 2004).

Fluorescence measurements in the light

Fluorescence parameters were measured during illumination from *Synechocystis* cells (optical density at 730 nm 0.8–1.1), pumpkin thylakoids (100 μg Chl ml^{-1}), and detached pumpkin leaves with a PAM-2000 (Walz, Effeltrich, Germany) at 5–35°C. A saturating pulse was fired to calculate $(F_M - F_0)/F_M$ $(=F_V/F_M)$ after dark acclimation (30 s for thylakoids and 30 min for

leaves). Thereafter, the sample was illuminated with white light (PPFD 750 μmol m^{-2} s^{-1} from a slide projector for *Synechocystis*, and PPFD 1500 μmol m^{-2} s^{-1} from a 500 W high-pressure xenon lamp with a water filter for pumpkin; for the spectra, see Fig. S1). To calculate $(F_M' - F)/F_M'$, saturating pulses were fired after 1 min for thylakoids and after 15, 30, and 45 min for *Synechocystis* cells and pumpkin leaves. To estimate the reduction state of Q_A, 1 − qL (Kramer *et al.*, 2004) was calculated, using an estimation (Oxborough & Baker, 1997) for F_0' (see Mattila *et al.*, 2020).

Photoinhibition treatments

Pumpkin thylakoids (100 μg Chl ml^{-1}), detached pumpkin leaves, or intact *Synechocystis* cells (optical density at 730 nm 0.8–1.1) were illuminated at various PPFD values, wavelengths, and temperatures, as indicated. Before a treatment, leaves were incubated overnight at PPFD 10–20 μmol m^{-2} s^{-1} with the petioles in a solution with 0.4 mg ml^{-1} lincomycin (Sigma-Aldrich). Lincomycin (0.4 mg ml^{-1}) was added to *Synechocystis* cells right before the treatment. Thylakoids were illuminated in photoinhibition buffer, unless otherwise mentioned, and *Synechocystis* cells in BG-11. The samples were mixed during the treatments. Red (> 650 nm) or blue (400–450 nm) light was obtained with a 500 W high-pressure xenon lamp equipped with a long-pass or a short-pass edge filter (LL-650 and LS-450, respectively; Corion, Holliston, MA, USA). Monochromatic light was obtained with band-pass filters (full width at half maximum 10 nm; Corion; Newport, Irvine, CA, USA). UV radiation was obtained with VL-8.LC (365 and 254 nm) and VL-8.M (312 nm) lamps (Vilber Lourmat, Collégien, France; for the spectra, see Havurinne *et al.*, 2021). White light was obtained from a 1000 W (Sciencetech, London, ON, Canada) or 500 W (Oriel Instruments; Newport) high-pressure xenon lamp (when measuring the temperature dependence of photoinhibition in thylakoids at 5°C intervals, and for the temperature dependence of photoinhibition in leaves), from a slide projector equipped with a low-voltage halogen lamp (*Synechocystis*), or from a 10 W cold-white LED (all other experiments). For laser-pulse-induced photoinhibition, pumpkin thylakoids (27 μl, 76 μg Chl ml^{-1}) were illuminated in a 3 × 3 × 10 mm^3 cuvette with 532 nm, 4 ns, 12.5 mJ pulses from a Nd : YAG laser (Continuum, San Jose, CA, USA). The interval between the laser pulses was 0.1 s (240 flashes in total), 10 s (100 flashes) or 30 s (40 flashes).

α-Tocopherol, when used, was vigorously mixed in dimethyl sulfoxide and immediately added to thylakoid suspension, which was then vigorously mixed for 20 s. In control experiments, only dimethyl sulfoxide was added. Anaerobic conditions, applied when indicated, were achieved by flushing the sample continuously with nitrogen (N_2) gas. In control (aerobic) experiments, the sample was flushed with air. Freshly prepared 20 mM sodium bicarbonate was used to test recovery of PSII activity in isolated thylakoids after anaerobic photoinhibition.

Experiments with isolated thylakoids were always repeated under otherwise identical conditions in the dark, to determine the rate of dark inactivation of PSII.

Quantification of photoinhibition

Before and after treatments, light-saturated O_2 evolution was measured from aliquots of treated thylakoids or from thylakoids isolated from treated leaves, at 22°C, or from aliquots of illuminated *Synechocystis* suspension at 32°C, using an O_2 electrode (Hansatech, King's Lynn, UK) as previously described (Hakala *et al.*, 2005) with artificial electron acceptors (0.5 mM 2,6-dimethylbenzoquinone (DMBQ) with thylakoids; 0.5 mM 2,6-dichlorobenzoquinone and 0.5 mM hexacyanoferrate(III) with *Synechocystis*). In some experiments, as indicated, PSII activity was estimated by measuring the fluorescence parameter F_V/F_M with a Fluorpen (Photon Systems Instruments, Brno, Czech Republic) after at least 5 min (thylakoids) or 30 min (leaves) dark incubation.

The rate constant of photoinhibition k_{PI} was calculated by fitting the loss of O_2 evolution or decrease in F_V/F_M, as indicated, to the first-order reaction equation in SIGMAPLOT (Systat Software Inc., Palo Alto, CA, USA). In the case of thylakoids, the final k_{PI} values were obtained by subtracting the first-order rate constant of dark inactivation from the raw k_{PI} value.

Activation energy

The activation energy E_a was calculated by fitting the dependence of the rate constant k on absolute temperature T to the Arrhenius equation by using linear regression of $\log_e(k)$ to $1/T$ according to the equation $\log_e(k) = -E_a/(k_b T)$ + constant, where k_b is Boltzmann's constant.

Detection of carbon-centered radicals

We mixed 5.9 mg of α-(4-pyridyl 1-oxide)-*N*-*tert*-butylnitrone (POBN; Enzo Life Sciences Inc., New York, NY, USA) in 0.6 ml of thylakoid suspension (100 μg Chl ml^{-1}) to get a final concentration of 50 mM POBN. POBN-R-adduct (the reaction product of POBN and a carbon (C)-centered radical) was detected before and immediately after illumination or dark incubation with an EPR spectrometer (Miniscope MS 5000; Magnettech GmbH, Berlin, Germany). The measurement parameters were as follows: 60 s sweep time (three technical repetitions) at 330–340 mT, 0.2 mT modulation, 100 kHz frequency, and 10 mW power. C-centered radicals were quantified by the height of the first positive peak at 334.5–334.8 mT of the EPR signal.

Results

Singlet oxygen production by thylakoid membranes shows a positive temperature dependence

Isolated pumpkin thylakoids were illuminated in high light at −2, 5, 15, 25, and 35°C, and $^1O_2$ production during the illumination was measured with the histidine method (Rehman *et al.*, 2013). $^1O_2$ production increased five-fold from −2 to +35°C, and the data showed a reasonable fit to the Arrhenius equation (Fig. 1). The reaction between $^1O_2$ and histidine,

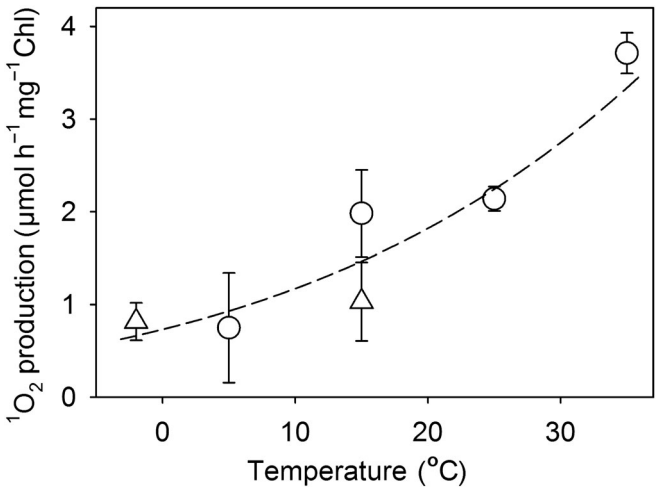

Fig. 1 Temperature dependence of singlet oxygen ($^1O_2$) production under intense white light by isolated pumpkin thylakoids, measured with a histidine-based method. Oxygen (O_2) was measured with an optode (circles) or with an O_2 electrode (triangles). The measurement device was calibrated in water (circles) or in the photoinhibition buffer (triangles). The data measured at photosynthetic photon flux density (PPFD) 3000 μmol m^{-2} s^{-1} (triangles) have been normalized to PPFD 2000 μmol m^{-2} s^{-1} by multiplying by 2/3. Each data point represents an average of at least three independent measurements, and the error bars show SDs. The dashed line shows the best fit to the Arrhenius equation, revealing an E_a of 0.31 eV.

probed by using rose bengal as a $^1O_2$ sensitizer, showed much weaker temperature dependence (Fig. S2), indicating that the temperature dependence in Fig. 1 reflects the temperature dependence of $^1O_2$ production by thylakoids and not that of the reaction between $^1O_2$ and histidine.

Temperature dependence of singlet oxygen production matches that of the misses

Photosystem II is responsible for most $^1O_2$ produced by thylakoids (Cazzaniga *et al.*, 2012). However, to understand which PSII charge recombination reaction is responsible for the $^1O_2$ production, the temperature dependences of recombination reactions were compared with the observed temperature dependence of $^1O_2$ formation. The sub-nanosecond recombination of $P_{680}^+Pheo^-$ is known to occur readily even at 77 K (Zabelin *et al.*, 2016), indicating negligible E_a, and the triplet state $^3P_{680}$ has only *c.* 0.025 eV lower energy than the $P_{680}^+Pheo^-$ radical pair (Dau & Zaharieva, 2009), implying that the temperature dependence of triplet formation via recombination right after primary charge separation is negligible at physiological temperatures. Therefore, rapid recombination of the primary pair does not account for the observed $^1O_2$ formation by PSII.

Next, recombination of the charge pairs consisting of a reduced quinone acceptor (Q_A^- or Q_B^-) and a hole in the OEC in the state S_2 were studied with thermolumiscence. The rate constants of the $S_2Q_A^- \rightarrow S_1Q_A$ and $S_2Q_B^- \rightarrow S_1Q_B$ recombination reactions can be calculated from the thermoluminescence Q (with DCMU) and B (no DCMU) bands, respectively. Previously, it has been shown that three competing pathways operate for the $S_2Q_A^- \rightarrow S_1Q_A$ recombination (Rappaport & Lavergne, 2009). The 'excitonic' pathway leads, via $P_{680}^+Pheo^-$, to the short-lived singlet excited state of P_{680} and produces the luminescence. The 'indirect' pathway also has the primary pair as an intermediate; it does not produce luminescence but can instead lead to the formation of $^3P_{680}$ when the $P_{680}^+Pheo^-$ pair recombines. The third, also non-luminescent, pathway has been interpreted as direct recombination of a hole in the OEC and an electron in Q_A^- without the primary pair as an intermediate (Rappaport & Lavergne, 2009).

The Q band peaked at 12°C and the B band at 37°C (Fig. 2a). We applied the model of Rappaport & Lavergne (2009) for the analysis of the Q band (see also Rantamäki & Tyystjärvi, 2011). For the B band, a first-order model with one recombining component (Randall & Wilkins, 1945; Tyystjärvi & Vass, 2004) was used. The rate constant of each pathway was obtained by fitting the curve to the respective model (Table S1). The rate constant of the indirect pathway of $S_2Q_A^-$ recombination ($k_{indirect}$) and the rate constant of $S_2Q_B^-$ recombination (the reactions that may lead to $^1O_2$ production) showed steep temperature dependences in the −2 to +35°C range (Fig. 2b). Such direct comparisons between the rate constant of recombination and $^1O_2$ formation are justified in isolated thylakoids in which PSII reaction centers would remain essentially closed during illumination, irrespective of the temperature (Fig. S3). In leaves, however, the rate of $^3P_{680}$ production from a recombination reaction under continuous illumination would be proportional to the rate constant of the recombination times the concentration of its substrate (a reduced quinone in this case). To measure the effect of temperature on the closure of PSII centers, we estimated the relative concentration of Q_A^-, $[Q_A^-]_{rel}$, at 5, 20, and 35°C, in pumpkin leaves using the fluorescence parameter 1 − qL (Figs 2c, S3). However, the product $k_{indirect} \times [Q_A^-]_{rel}$ showed a highly similar temperature dependence to the rate constant $k_{indirect}$ alone, much steeper than the temperature dependence of $^1O_2$ production (Fig. 2d). The temperature dependence of the rate constant of $S_2Q_B^-$ recombination (inset of Fig. 2b) was also steeper than that of $^1O_2$ formation; no correction for the *in vivo* rate of $S_2Q_B^-$ recombination was deemed necessary because Q_B is a two-electron carrier and therefore the concentration of Q_B^- would not depend strongly on temperature in continuous light. Thermoluminescence peaks originating from the recombination of the $S_3Q_A^-$ and $S_3Q_B^-$ states are not drastically different from those related to the S_2 state (Vass & Govindjee, 1996); recombination reactions involving the S_3 state instead of S_2 would therefore not change the conclusions drawn herein. The 'direct' pathway of $S_2Q_A^-$ recombination also contributed to our experimental data (Fig. 2b), but this pathway does not have a radical pair intermediate (Rappaport & Lavergne, 2009) and therefore cannot contribute to $^1O_2$ production. To summarize, the $S_{2/3}Q_{A/B}^- \rightarrow S_{1/2}Q_{A/B}$ recombination reactions cannot be the main producers of $^1O_2$ in thylakoids.

The temperature dependence of misses of OEC has been earlier measured from spinach thylakoids (Isgandarova *et al.*, 2003), and a comparison shows that the temperature dependence of

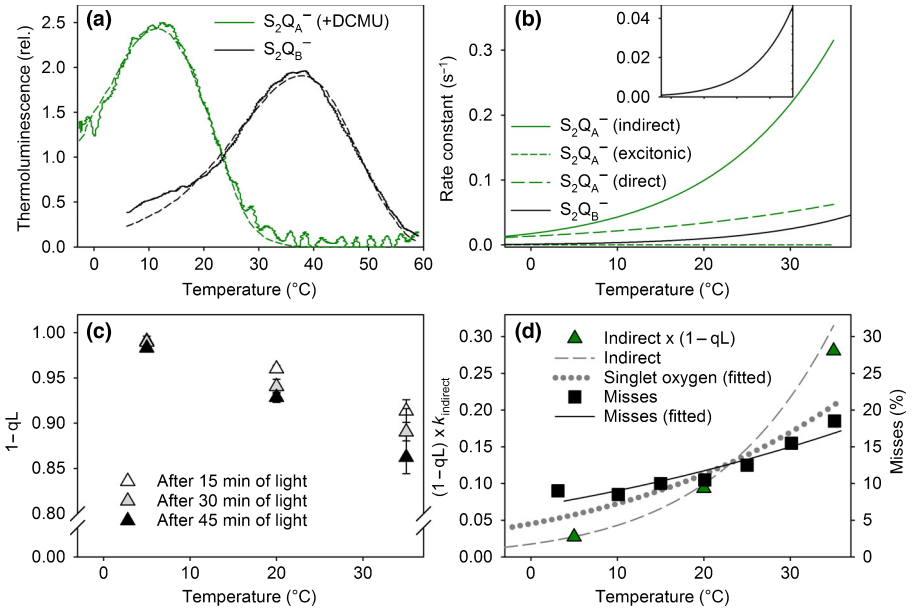

Fig. 2 Temperature dependences of charge recombination reactions and reduction state of Q_A. (a) Thermoluminescence Q (solid green line; in the presence of 3-(3,4-dichlorophenyl)-1,1-dimethylurea (DCMU)) and B (solid black line) bands were measured from isolated pumpkin thylakoid membranes after a xenon flash at −10°C. The underlying dashed lines show the best fits to a three-reaction model (Rappaport & Lavergne, 2009) for the Q band, and to the Randall & Wilkins (1945) model for the B band. Each experimental curve represents an average of three independent measurements. (b) Temperature dependences of the rate constants of the three routes of $S_2Q_A^-$ recombination (green continuous and dashed lines) and the $S_2Q_B^-$ recombination (black continuous line), calculated based on the thermoluminescence data in (a). The inset shows $S_2Q_B^-$ recombination in a narrower *y*-axis scale. (c) Temperature dependence of the fraction of closed photosystem II centers (Q_A^-), measured as the 1 − qL Chl *a* fluorescence parameter in pumpkin leaves after 15 min (white triangles), 30 min (light gray triangles), or 45 min (black triangles) illumination with white light (photosynthetic photon flux density 1500 μmol m^{-2} s^{-1}). Each data point represents an average of at least three independent measurements, and the error bars show SDs. (d) The rate constant of the indirect recombination ($k_{indirect}$) from (b) multiplied by (1 − qL) at 30 min from (c) (green triangles), and the temperature dependence of misses in spinach thylakoids (black squares), measured by Isgandarova *et al*. (2003). The underlying black line shows the best fit to the Arrhenius equation. The gray dashed line shows the temperature dependence of $k_{indirect}$ from (b), and the gray dotted line shows singlet oxygen production from Fig. 1, normalized to have the same intersection as the other curves, for comparison.

misses, especially at 10–35°C, is highly similar to that of $^1O_2$ production (Figs 1, 2d). These data suggest that $^1O_2$ is produced mainly via the miss-associated $P_{680}{}^+Q_A^-$ recombination reaction (see Discussion section for details).

Temperature dependence of photoinhibition is positive, universal among different species, and depends on the wavelength of illumination

Connections between $^1O_2$ and photoinhibition observed in previous literature – for a review, see Tyystjärvi (2013) – prompted us to compare their temperature dependences. The temperature dependence of photoinhibition was measured by illuminating isolated pumpkin thylakoids with strong white light at 3–35°C. The loss of light-saturated O_2 evolution (water (H_2O) to DMBQ), measured from aliquots of the treated suspension, was fitted to the first-order reaction equation (Fig. S4a) to obtain a raw rate constant, from which the rate constant of dark inactivation, occurring in isolated thylakoids, was subtracted to calculate the rate constant of photoinhibition k_{PI} (Fig. S4b). To ensure that the results are not a property of isolated systems only, the temperature dependence of photoinhibition was also measured *in vivo* by illuminating intact pumpkin leaves or cells of the cyanobacterium *Synechocystis* sp. PCC 6803 in the presence of lincomycin to block PSII repair (Fig. S4c). The data show an essentially identical, positive temperature dependence of photoinhibition for pumpkin thylakoids, *Synechocystis* cells, and pumpkin leaves; k_{PI} approximately doubled in the measured physiological temperature range (Fig. 3a). Furthermore, the temperature dependence of photoinhibition resembled those of misses and $^1O_2$ production (Fig. 2d).

Photoinhibition by strong nanosecond laser pulses has earlier been suggested to be caused by $^1O_2$ specifically originating from $S_2Q_A^-$ and $S_2Q_B^-$ recombination reactions (Keren *et al*., 1997). Measurements of laser-pulse-induced photoinhibition in pumpkin thylakoids (Fig. 3b) confirmed the characteristic dependence of the photoinhibitory efficiency (per flash) on the time interval between the flashes (Keren *et al*., 1997). However, comparison of Figs 1–3 shows that the temperature response of the laser-pulse-induced photoinhibition does not resemble the temperature dependence of any of the $S_2Q_A^-$ or $S_2Q_B^-$ recombination pathways, indicating that photoinhibition induced with short laser pulses is not related to these recombination reactions. In addition, the temperature dependence of laser-pulse-induced photoinhibition did not resemble that of photoinhibition induced by continuous light (Fig. 3a), suggesting a different photoinhibitory mechanism.

The resemblance of the temperature dependence of photoinhibition caused by continuous high-intensity white light (Fig. 3a)

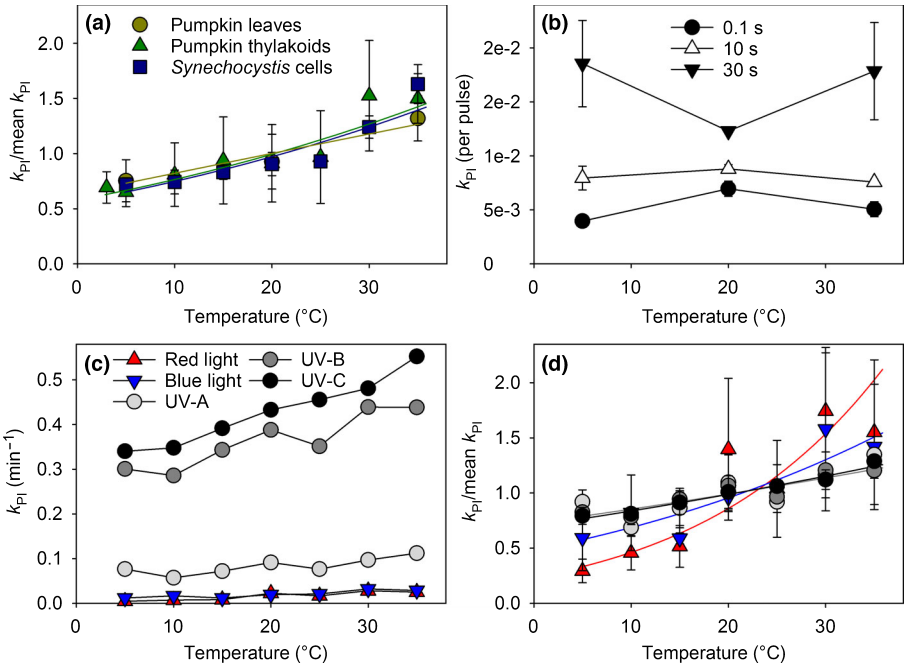

Fig. 3 Temperature dependence of photoinhibition. (a) Temperature dependences of rate constants of photoinhibition k_{PI} in lincomycin-treated pumpkin leaves (dark yellow circles), pumpkin thylakoids (green triangles), and lincomycin-treated *Synechocystis* cells (blue squares). Photoinhibition was caused by illumination with white light (photosynthetic photon flux density (PPFD) 1500 μmol m^{-2} s^{-1} for thylakoids and leaves, PPFD 750 μmol m^{-2} s^{-1} for *Synechocystis*). Symbols represent experimental data, and the underlying lines show the best fits to the Arrhenius equation. (b) Temperature dependence of photoinhibition induced by 4 ns, 532 nm laser pulses fired with intervals of 0.1 s (closed circles), 10 s (open triangles), or 30 s (closed triangles) in pumpkin thylakoids. (c, d) Temperature dependence of photoinhibition induced by red (red upward triangles) or blue (blue downward triangles) light (PPFD 1500 μmol m^{-2} s^{-1}), and by ultraviolet (UV)-A (light gray circles; PFD 300 μmol m^{-2} s^{-1}), UV-B (dark gray circles; PFD 500 μmol m^{-2} s^{-1}), or UV-C (black circles; PFD 300 μmol m^{-2} s^{-1}) radiation in pumpkin thylakoids. (d) Symbols represent experimental data, and the underlying lines show the best fits to the Arrhenius equation. The k_{PI} values were calculated by fitting the light-induced decline in the rate of light-saturated oxygen evolution of photosystem II (water to an artificial electron acceptor) to the first-order reaction equation, individually for each experiment. The symbols show average k_{PI} values, based on at least three measurements, and error bars, drawn if larger than the symbol, show SDs, except for (b) where fitting was done on the averaged data; error bars show the SE of the fit. See Supporting Information Fig. S4 for details. In (a) and (d), the k_{PI} values have been normalized to their respective average values to facilitate comparison.

with those of misses and $^1O_2$ production (Fig. 2d) suggests, in turn, that the miss-associated recombination reaction leads to the production of $^1O_2$, which then damages PSII. As $^1O_2$ is not produced under UV radiation (Hideg & Vass, 1996), we tested whether the temperature dependence of photoinhibition would be lost in UV radiation. Different wavelengths of visible light were also tested. As shown previously (e.g. Hakala *et al.*, 2005), the k_{PI} value, when compared with photon flux density, is much higher under UV radiation than under visible light (Fig. 3c). Normalized data show that the positive temperature dependence remains, although it is somewhat milder in UV than in visible wavelengths, especially than in red light (Fig. 3d).

Photoinhibition proceeds similarly under aerobic and anaerobic conditions

Besides UV illumination, anaerobicity is a condition where photoinhibition has been previously shown to occur even though $^1O_2$ is not produced. Therefore, to better understand the connection between $^1O_2$ production and photoinhibition, we next illuminated thylakoids in anaerobic conditions. In this case, photoinhibition was assayed with the F_V/F_M fluorescence parameter. As shown by Sipka *et al.* (2021), F_V/F_M cannot be taken as a measure of the PSII quantum yield but can be used as an empirical PSII activity parameter. The experiments showed an essentially similar temperature dependence of photoinhibition under anaerobic and aerobic conditions (Fig. 4a). The action spectrum, another characteristic of the reaction mechanism, was similar for anaerobic and aerobic photoinhibition (Fig. 4b).

Photoinhibition *in vitro* can be reversible under anaerobic conditions, mainly because of depletion and rebinding of bicarbonate to PSII (Sundby *et al.*, 1992). However, we did not observe any reversibility, nor did addition of bicarbonate affect photoinhibition (Fig. S5).

To further test the effect of $^1O_2$ production on photoinhibition, we illuminated pumpkin thylakoids in the presence of two efficient $^1O_2$ scavengers, water-soluble histidine and hydrophobic α-tocopherol, and found no effect on photoinhibition or on its temperature dependence (Fig. 4c). In the dark, these compounds did not show any clear effects either, except small protection by histidine against light-independent inactivation of PSII (Fig. S6). These results show that either photoinhibition is independent of $^1O_2$ or has parallel mechanisms, some of them independent of O_2.

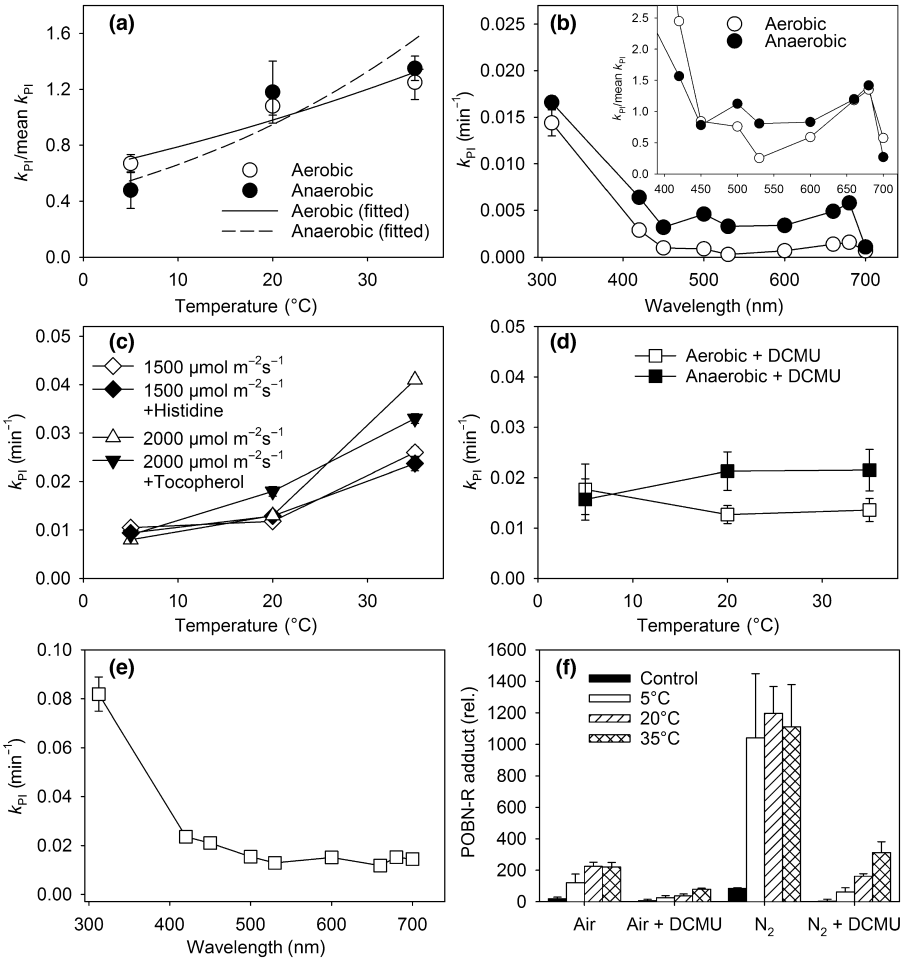

Fig. 4 Photoinhibition in pumpkin thylakoids under anaerobic conditions, in the presence of 3-(3,4-dichlorophenyl)-1,1-dimethylurea (DCMU) and quenchers of singlet oxygen (O_2). (a) Temperature dependence and (b) action spectrum of photoinhibition under aerobic (constant air bubbling; open circles) and anaerobic (constant nitrogen (N_2) bubbling; closed circles) conditions. In (a) and in the inset showing only the visible wavelength range in (b), the rate constants of photoinhibition k_{PI} have been normalized to their respective mean values. The photosynthetic photon flux densities (PPFDs) were (a) 1150 µmol m^{-2} s^{-1} of white light and (b) 400 µmol m^{-2} s^{-1} at indicated wavelengths. (c) Temperature dependence of photoinhibition induced with white light (PPFD 2000 or 1500 µmol m^{-2} s^{-1}, as indicated) under aerobic conditions in the absence (open diamonds) or presence of 5 mM histidine (closed diamonds), and in the absence (open upward triangles) or presence of 0.5 mM α-tocopherol (closed downward triangles). (d) Temperature dependence and (e) action spectrum of photoinhibition in the presence of DCMU under aerobic (constant air bubbling; open squares) and anaerobic (constant N_2 bubbling; closed squares) conditions at (d) PPFD 1150 µmol m^{-2} s^{-1} of white light and (e) 400 µmol m^{-2} s^{-1} at indicated wavelengths. In (e) photosystem II activity was assayed with O_2 evolution (water to an artificial electron acceptor); in (a), (b), (d), and (e), the fluorescence parameter F_V/F_M was used. In (a), the symbols show average k_{PI} values, based on at least three measurements, and error bars show SDs. In (b–e), fitting was done on the averaged data (of at least three independent experiments); error bars, drawn when larger than the symbol, show the SE of the fit. (f) Temperature dependence of production of carbon-centered radicals, in the presence or absence of O_2 (constant air or nitrogen bubbling), and in the presence or absence of DCMU, as indicated, by pumpkin thylakoids illuminated with white light, PPFD 2000 µmol m^{-2} s^{-1}, in the presence of α-(4-pyridyl 1-oxide)-*N*-*tert*-butylnitrone (POBN). The reaction product of POBN and the radicals (POBN-R adduct) was quantified by electron paramagnetic resonance. Closed bars represent the amount of the POBN-R adduct before the light treatment (control). Each bar represents an average of at least three independent experiments, and error bars show SDs.

We also measured aerobic and anaerobic photoinhibition in the presence of DCMU, a herbicide that blocks electron transfer from Q_A to Q_B. Again, photoinhibition was measured with F_V/F_M. Interestingly, in the presence of DCMU, the temperature dependence was lost (Fig. 4d), and in the visible range the action spectrum was flatter than in the absence of DCMU (Fig. 4e). Owing to a relatively low resolution, we may have missed a previously observed peak at 670 nm (Santabarbara *et al.*, 2001).

Photoinhibition proceeded faster in anaerobic than in aerobic conditions (Fig. 4b). To test whether accumulation of C-centered radicals would explain this result, we illuminated pumpkin thylakoids in the presence of the radical probe POBN and found more radicals after anaerobic than after aerobic illumination (Fig. 4f). However, accumulation of radicals did not show a clear temperature dependence at 5–35°C in the absence of DCMU (Fig. 4f), contrary to photoinhibition. Both in the presence and absence of O_2, DCMU strongly suppressed radical accumulation but, curiously, also imposed a positive temperature dependence (Fig. 4f). Accumulation of C-centered radicals was negligible in the dark at 20°C, and the signal,

obtained by illumination, remained stable in the dark at 5–35°C (Fig. S7).

A connection between misses and photoinhibition was further probed by comparing the pH dependences of the two phenomena. The k_{PI} value decreased by one-third from pH 6.8 to pH 8.2 (Fig. S8), whereas misses show little pH dependence in this range (Messinger & Renger, 1994). However, Davletshina & Semin (2020) have suggested that the pH dependence of photoinhibition may reflect pH-dependent changes in the structure of the OEC. These changes may affect photoinhibition without affecting the miss rate.

Temperature of dark incubation affects fluorescence-based estimations of photoinhibition

Finally, we assayed photoinhibition in pumpkin leaves both with F_V/F_M and O_2 evolution. A similar positive temperature dependence was obtained irrespective of the assay method (Fig. S9a). However, if the 30 min dark incubation before the F_V/F_M measurement was conducted at 5°C (the illumination temperature), photoinhibition appeared to proceed faster than when the dark incubation was done at 22°C (Fig. S9b). Thus, dark-incubation temperature may greatly affect the extent of the observed decline in F_V/F_M.

Discussion

Miss-associated recombination of $P_{680}{}^+Q_A{}^-$ is responsible for singlet oxygen production of photosystem II

In plants, chloroplasts are the most important producers of $^1O_2$ in the light (Hideg *et al.*, 2002; Prasad *et al.*, 2018), and the potential of $^3P_{680}$ for the $^1O_2$ production has been clear for many years (Telfer *et al.*, 1994). $^3P_{680}$ is produced by charge recombination reactions, but the importance of different recombination pathways has not been known. It has been suggested that $S_nQ_{A/B}{}^- \rightarrow S_{n-1}Q_{A/B}$ reactions produce enough $^3P_{680}$ and subsequently $^1O_2$ to inactivate PSII in weak light or during illumination with short laser pulses (Keren *et al.*, 1997; Vass, 2011). The recombination of $P_{680}{}^+Pheo^-$ has been suggested to be important in $^1O_2$ production in strong light when Q_A is mostly reduced (Vass, 2011; Rehman *et al.*, 2013). Our data show that these recombination reactions cannot significantly contribute to $^1O_2$ production; the temperature dependences of the slow recombinations are too steep and that of the rapid recombination of the primary radical pair is too flat to account for the observed temperature dependence of $^1O_2$ formation by thylakoid membranes (Figs 1, 2). Furthermore, $^3P_{680}$ is short-lived in the presence of $Q_A{}^-$ (Hillmann *et al.*, 1995; Santabarbara *et al.*, 2003).

The miss-associated recombination of $P_{680}{}^+Q_A{}^-$ is the only reaction with a temperature response similar to the observed $^1O_2$ production (Figs 1, 2), and therefore the data strongly suggest that $^1O_2$ is produced in a reaction between O_2 and $^3P_{680}$, where $^3P_{680}$ is formed by the miss-associated recombination of $P_{680}{}^+Q_A{}^-$ (see Fig. 5a). This reaction, like all recombination reactions of PSII (except for the recombination of the primary pair), is expected to have a high triplet yield because of the lack of spin correlation of the reactants.

Energetics of misses, recombination reactions, and singlet oxygen formation

The miss-associated recombination of $S_1P_{680}{}^+Q_A{}^-$ would obviously proceed via pathways equivalent to the reducing side of the indirect and excitonic pathways of $S_2Q_A{}^-$ recombination (Rappaport & Lavergne, 2009); that is, via the $S_1P_{680}{}^+Pheo^-Q_A$ intermediate. Assuming that the pre-exponential factor s takes similar values in $P_{680}{}^+Q_A{}^-$ recombination as in $S_2Q_A{}^-$ recombination (Table S1), and knowing that the Gibbs energy change from $P_{680}{}^+PheoQ_A{}^-$ to $P_{680}{}^+Pheo^-Q_A$ is 0.33 eV (Dau & Zaharieva, 2009), the time constant of the recombination reaction $P_{680}{}^+PheoQ_A{}^- \rightarrow P_{680}{}^+Pheo^-Q_A$ (which may lead to $^3P_{680}$) would be 191 μs at 25°C (see Calculations in Methods S1), in agreement with the time constant of 100–200 μs, measured by Renger & Wolff (1976).

A miss of the OEC occurs because the S-state does not always advance, not because the recombination of $P_{680}{}^+Q_A{}^-$ occasionally wins competition with normal advancement of the S-state (Pham *et al.*, 2019). The simplest mechanism by which misses can originate from the oxidizing side of PSII is that the OEC has a miss-prone state (OEC_{miss}), characterized by a slow $S_n \rightarrow S_{n+1}$ transition. Thus, the temperature dependence of $^1O_2$ formation reflects the activation energies of a multistep reaction beginning with the reaction $OEC_{normal} \rightarrow OEC_{miss}$, which, based on analysis of the results of Isgandarova *et al.* (2003), has an E_a of 0.224 eV (Fig. 5b). This E_a is the enthalpy difference between the transition state of the reaction $OEC_{normal} \rightarrow OEC_{miss}$ and OEC_{normal}. If we assume that the miss factor is 8% at 25°C and all misses occur in the $S_2 \rightarrow S_3$ transition, then the equilibrium constant of the reaction $OEC_{normal} \rightarrow OEC_{miss}$ is 0.32. As $K_{eq} = e^{-\Delta G_r/k_bT}$, where ΔG_r is the Gibbs energy change of the reaction, this further implies that OEC_{miss} is 0.03 eV above OEC_{normal}.

After a charge separation and reduction of Q_A, a multistep reaction forming $^1O_2$ consists of the reaction $OEC_{normal} \rightarrow OEC_{miss}$, recombination $P_{680}{}^+Q_A{}^- \rightarrow P_{680}Q_A$, formation of $^3P_{680}$, and a reaction between O_2 and $^3P_{680}$ (Fig. 5a). An effective E_a of a multistep reaction is calculated by adding k_bT and the sum of the standard-state enthalpies (subtracting those of the reactants) of all intermediates and transition states of the reaction, where each enthalpy value is multiplied by its degree of rate control (DRC) (Mao & Campbell, 2019). The radical pair $P_{680}{}^+Pheo^-$ represents the transition state of the $P_{680}{}^+Q_A{}^- \rightarrow P_{680}Q_A$ recombination reaction, which implies that the E_a of the recombination reaction is the same as the redox potential difference of the Pheo/$Pheo^-$ and $Q_A/Q_A{}^-$ pairs, 0.33 eV (Dau & Zaharieva, 2009). A slightly smaller E_a of $^1O_2$ formation, 0.31 eV (Fig. 5b), indicates that contributions from the formation of $^3P_{680}$ and the reaction between O_2 and $^3P_{680}$ to the E_a are close to zero. Indeed, formation of $^3P_{680}$ occurs even at 10 K (Lendzian *et al.*, 2003), indicating that the triplet formation does not depend on temperature at 2–35°C. $^1O_2$ production by

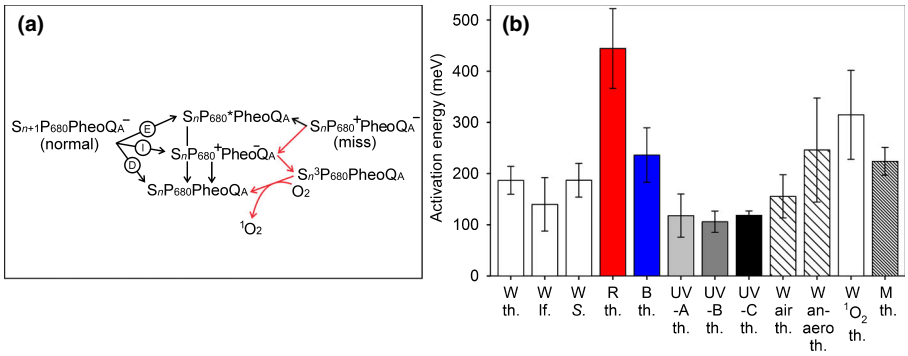

Fig. 5 Activation energies and recombination pathways. (a) Recombination pathways of photosystem II (PSII). A charge separation produces either reduction of Q_A and advancement of the S-state of oxygen (O_2) evolving complex (normal) or reduction of Q_A without advancement of the S-state (miss). The three charge recombination pathways from the 'normal' state are depicted as direct (D), indirect (I), and excitonic (E). The excited triplet state of the PSII reaction center Chl(s) $^3P_{680}$ can be produced either from the indirect (via the primary charge pair $P_{680}{}^+Pheo^-$) recombination pathway or equivalent recombination from the miss configuration, but the miss recombination (red arrows) is much faster and has a temperature dependence matching singlet O_2 ($^1O_2$) production. (b) Activation energy of photoinhibition in pumpkin thylakoids (th.), pumpkin leaves (lf.), and *Synechocystis* cells (*S.*), obtained under illumination in white (W), blue (B), or red (R) light and in ultraviolet (UV)-A, UV-B, or UV-C radiation, measured using O_2 evolution as a PSII activity assay. Activation energy of photoinhibition in aerobic (air; as a control) and anaerobic (anaero) conditions, quantified using the fluorescence parameter F_V/F_M as a PSII activity assay (sparsely hatched bars). Activation energy of $^1O_2$ production, measured with a histidine-based method. Activation energy of the miss factor of spinach thylakoids (M; densely hatched bars), calculated from published data (Isgandarova *et al.*, 2003). Error bars show the SEs. Original data are from Figs 1–4. The rates of the reactions have different units, but calculation of activation energies is independent of the unit. For the fits to the Arrhenius equation, see Figs 1, 3, 4.

illuminated rose bengal, in turn, has an activation energy of only 0.055 eV (Fig. S2b). This E_a belongs to a complicated reaction in which the conversion of $^1O_2$ to O_2 via collision of H_2O competes with the reaction of $^1O_2$ with histidine. We now assume that the products DRC × E_a for the reactions between $^3P_{680}$ and O_2, followed by the reaction between $^1O_2$ and histidine, are negligible because these reactions occur after $^1O_2$ formation and because the E_a contribution of this series of steps would be comparable to the small E_a measured for the production and detection of $^1O_2$ in the rose bengal system. With these assumptions, direct application of the model of Mao & Campbell (2019) for the measured E_a of $^1O_2$ formation results in $E_a(^1O_2) = k_bT +$ DRC1 × 0.224 eV + DRC2 × 0.03 eV + DRC3 × 0.33 eV = 0.31 eV, where DRC1 belongs to the moving of the reaction coordinate from OEC_{normal} to the transition state of the reaction $OEC_{normal} \rightarrow OEC_{miss}$, DRC2 belongs to the formation of OEC_{miss} from the transition state, and DRC3 belongs to the transitional step $P_{680}{}^+PheoQ_A{}^- \rightarrow P_{680}{}^+Pheo^-Q_A$. We further assume that DRC2 is zero, and, taking into account that DRC1 + DRC2 + DRC3 = 1, we get DRC1 = 0.39 and DRC3 = 0.61 (calculations in Methods S1). Thus, the rate of $^1O_2$ formation is controlled both by the frequency of misses and by the rate of the miss-associated recombination reaction.

Photoinhibition has three parallel mechanisms

Our data conclusively show that the temperature dependence of photoinhibition is positive both *in vivo* and *in vitro*. The result agrees with several earlier studies (Tyystjärvi *et al.*, 1994; Lazarova *et al.*, 2014; Ueno *et al.*, 2016; Mattila *et al.*, 2020) but contrasts with the findings of Tsonev & Hikosaka (2003) and Kornyeyev *et al.* (2003), who found a strong negative temperature dependence. The difference might suggest that, in our experiments, excitation pressure (suggested to be the cause of fast photoinhibition at low temperatures) was similar at all temperatures. Though this actually is true for the *in vitro* results (Fig. S3), the PSII yield of pumpkin leaves showed a clear negative dependence on temperature, indicating decreased excitation pressure at higher temperatures (Fig. 2c). Furthermore, no connection between excitation pressure and k_{PI} at different temperatures was found in our earlier study (Mattila *et al.*, 2020). A possible reason why Tsonev & Hikosaka (2003) and Kornyeyev *et al.* (2003) observed a negative temperature dependence for photoinhibition is that they used the Chl fluorescence parameter F_V/F_M for quantification of PSII activity. A low temperature during dark incubation between illumination and fluorescence measurement can affect the results by slowing the relaxation of nonphotochemical fluorescence quenching (Fig. S9); Tsonev & Hikosaka (2003) indeed performed the dark incubation and photoinhibition treatment at the same temperature.

$^1O_2$ has often been suggested to function as a causal agent of photoinhibition (Vass, 2011; Tyystjärvi, 2013), but the occurrence of photoinhibition under UV radiation and in anaerobic conditions where $^1O_2$ is not formed indicates that parallel mechanisms must function. We will first treat the visible-light-specific photoinhibition mechanisms as one combined mechanism functioning parallel with another mechanism that is fully responsible for photoinhibition under UV radiation. The apparent E_a of photoinhibition, in the presence of two parallel pathways, is the weighted sum, calculated as $E_a(\text{total}) = (k_1E_1 + k_2E_2)/(k_1 + k_2)$, where k_i and E_i are the rate constant and E_a of reaction i (i = 1, 2), respectively. As k_{PI} is proportional to photon flux density (Tyystjärvi & Aro, 1996), we can simplify the equation by the normalization $k_1 + k_2 = 1$.

We assume that the UV mechanism is triggered by light absorption by the Mn ions of OEC (Hakala *et al.*, 2005) and first calculate the contribution of the Mn mechanism in visible light. Absorbance values of Mn complexes decrease with wavelength (e.g. Horner *et al.*, 1999), and the contribution of the Mn mechanism is likely to be negligible in long-wavelength (red) visible light (Hakala *et al.*, 2005; Ohnishi *et al.*, 2005). We therefore postulate that photoinhibition in red light is entirely caused by mechanism(s) dependent on the light absorption by Chls, whose combination consequently must have an apparent E_a of 0.46 eV (Fig. 5b). If photoinhibition of thylakoids in white light (E_a 0.20 eV) is a linear combination of the UV mechanism (E_a 0.12 eV in UV-A) and the mechanism(s) functioning in red light, then the Mn mechanism contributes 76% in white and 65% in blue light. For more details, see Calculations in Methods S1. Such a high contribution of a mechanism that is independent of Chl absorption agrees with the relatively small protective effect of nonphotochemical quenching of Chl excitations (Sarvikas *et al.*, 2006; Havurinne & Tyystjärvi, 2017), although it can also be explained by assuming involvement of uncoupled Chls in photoinhibition (Santabarbara *et al.*, 2001). The mechanistic details of the Mn mechanism, except for the release of Mn ions from OEC (Hakala *et al.*, 2005), are still obscure, and therefore a dependence from O_2 or involvement of reactive O_2 species in the Mn mechanism cannot be excluded. However, photoinhibition induced by UV-A radiation was only weakly affected by removal of O_2 (Fig. 4b).

The fact that visible light induces photoinhibition in anaerobic conditions indicates that a $^1O_2$-independent mechanism must exist. The Mn mechanism cannot explain all such photoinhibition because the E_a of anaerobic photoinhibition in visible light is 0.26 eV whereas that of the UV-active mechanism is 0.12 eV. The effect of O_2 on the rate of photoinhibition in UV radiation and visible light can be used to estimate the importance of the Mn mechanism in anaerobic conditions in visible light. The ratio k_{PI}(anaerobic)/k_{PI}(aerobic) is, on average, 3.45 in visible light but only 1.2 at 312 nm (Fig. 4b), suggesting that anaerobicity does not boost the Mn mechanism and thus that all increase in the rate of photoinhibition due to lack of O_2 is accounted by an O_2-independent visible-light-specific mechanism. Following this assumption, the Mn mechanism, accounting for 76% of visible-light photoinhibition in aerobic conditions, only contributes by 22% in anaerobic conditions. Now, the E_a of the O_2-independent visible-light mechanism, functioning in parallel to the Mn mechanism, becomes $(0.26\ \text{eV} - 0.22 \times 0.12\ \text{eV})/0.78 = 0.30$ eV, which is somewhat but not drastically higher than the E_a of the misses (see Calculations in Methods S1), suggesting a causal relationship between misses and the O_2-independent mechanism. We suggest that the O_2-independent mechanism is the classical donor-side photoinhibition (Callahan & Cheniae, 1985; Chen *et al.*, 1992; Jegerschöld & Styring, 1996), in which P_{680}^+, if long-lived, commits a harmful oxidation in PSII. Misses, by prolonging the lifetime of P_{680}^+ by barring electron flow from OEC, may trigger this reaction in healthy PSII. If the miss-associated recombination has a time constant of 191 μs while electron transfer from Q_A^- to Q_B takes 500 μs, then the miss mechanism would prolong the lifetime of P_{680}^+ in 38% of the cases because electron transfer from Q_A^- to Q_B occurs before the miss-associated $P_{680}^+Q_A^-$ recombination. Thus, electron transfer from Q_A^- to Q_B after a miss would lock PSII to the P_{680}^+ state until the missed OEC finally advances the S-state.

The enhanced formation of C-centered radicals in anaerobic conditions (Fig. 4f) may suggest that oxidation of PSII proteins by P_{680}^+ is linked to anaerobic photoinhibition. In line with this suggestion, DCMU strongly suppressed radical formation. However, anaerobic photoinhibition is not suppressed by DCMU, indicating that not all protein oxidation events lead to loss of PSII activity; DCMU may alter the probabilities of different oxidation events. The lack of matching temperature dependence in radical formation and photoinhibition responses (Fig. 4d,f) confirms that the relationship between photoinhibition and formation of protein radicals is not straightforward.

The relative rates of the $^1O_2$-dependent and O_2-independent visible-light-specific mechanisms in the presence of O_2 cannot be estimated from the present data, but the E_a of their combination, 0.46 eV, and that of the O_2-independent reaction, 0.30 eV, imply that the E_a of the $^1O_2$-dependent mechanism is ≥ 0.46 eV. The strong photoprotective effect of carotenoids (Jahns *et al.*, 2000; Hakkila *et al.*, 2013) suggests that the $^1O_2$-dependent mechanism is the major contributor among the Chl-dependent mechanisms. Owing to the high E_a value of $^1O_2$-dependent photoinhibition, the relative contribution of this mechanism is expected to increase with temperature. This may explain why studies with cyanobacteria and algae that are cultivated and treated with high light in their cultivation temperature often yield results supporting the importance of $^1O_2$ (Jahns *et al.*, 2000; Fufezan *et al.*, 2007; Hakkila *et al.*, 2013; Treves *et al.*, 2016), whereas the results of the present study (mostly conducted on plant thylakoids) suggest a large contribution of the Mn mechanism that has a low E_a.

Temperature dependence may not exactly reflect E_a for PSII charge recombination reactions with tunneling character (Moser *et al.*, 2005). The good fit of the thermoluminescence data (Fig. 2a) may suggest that E_a is not damped, but the accuracy of the photoinhibition data does not allow estimation of dampening of the activation. Furthermore, we cannot exclude the possibility that the matching temperature dependences are fortuitous. In particular, $^1O_2$ formation by uncoupled Chls (Santabarbara *et al.*, 2001, 2002, 2003) might have a temperature dependence matching that measured for $^1O_2$ (Fig. 1).

Acknowledgements

We thank Mikko Antinluoma and Nicolas Reynoud for assistance. This work was supported by the Academy of Finland (grants 333421 and 271832), the Vilho, Yrjö and Kalle Väisälä Foundation, Turku University Foundation (grant 12354), and the Emil Aaltonen Foundation. The work was conducted at the Molecular Plant Biology unit, which forms the PhotoSYN infrastructure of the University of Turku.

Author contributions

ET designed the research; HM and SM performed the research; ET and HM analyzed the data; HM, ET and TT wrote the paper with contribution from SM.

ORCID

Heta Mattila https://orcid.org/0000-0002-5071-9721
Esa Tyystjärvi https://orcid.org/0000-0001-6808-7470
Taina Tyystjärvi https://orcid.org/0000-0003-0591-8630

Data availability

Raw data are available in Mendeley Data (https://data.mendeley.com/datasets/sg4bbmnjvc/1).

References

Callahan FE, Cheniae GM. 1985. Studies on the photoinactivation of the water-oxidizing enzyme. I. Processes limiting photoactivation in hydroxylamine-extracted leaf segments. *Plant Physiology* **79**: 777–786.

Cazzaniga S, Li Z, Niyogi KK, Bassi R, Dall'Osto L. 2012. The Arabidopsis szl1 mutant reveals a critical role of b-carotene in photosystem I photoprotection. *Plant Physiology* **159**: 1745–1758.

Chen G-X, Kazimir J, Cheniae GM. 1992. Photoinhibition of hydroxylamine-extracted photosystem II membranes: studies of the mechanism. *Biochemistry* **31**: 11072–11083.

Crawford T, Lehotai N, Strand Å. 2018. The role of retrograde signals during plant stress responses. *Journal of Experimental Botany* **69**: 2783–2795.

Dau H, Zaharieva I. 2009. Principles, efficiency, and blueprint character of solar-energy conversion in photosynthetic water oxidation. *Accounts of Chemical Research* **42**: 1861–1870.

Davis GA, Kanazawa A, Schöttler MA, Kohzuma K, Froehlich JE, Rutherford AW, Satoh-Cruz M, Minhas D, Tietz S, Dhingra A *et al.* 2016. Limitations to photosynthesis by proton motive force-induced photosystem II photodamage. *eLife* **5**: e16921.

Davletshina LN, Semin BK. 2020. pH dependence of photosystem II photoinhibition: relationship with structural transition of oxygen-evolving complex at the pH of thylakoid lumen. *Photosynthesis Research* **145**: 135–143.

Di Mascio P, Martinez GR, Miyamoto S, Ronsein GE, Medeiros MHG, Cadet J. 2019. Singlet molecular oxygen reactions with nucleic acids, lipids, and proteins. *Chemical Reviews* **119**: 2043–2086.

Forbush B, Kok B, McGloin M. 1971. Cooperation of charges in photosynthetic oxygen evolution-II. Damping of flash yield oscillation, deactivation. *Photochemistry and Photobiology* **14**: 307–321.

Fufezan C, Gross CM, Sjödin M, Rutherford AW, Krieger-Liszkay A, Kirilovsky D. 2007. Influence of the redox potential of the primary quinone electron acceptor on photoinhibition of photosystem II. *Journal of Biological Chemistry* **282**: 12492–12502.

Fufezan C, Rutherford AW, Krieger-Liszkay A. 2002. Singlet oxygen production in herbicide-treated Photosystem II. *FEBS Letters* **532**: 407–410.

Hakala M, Tuominen I, Keränen M, Tyystjärvi T, Tyystjärvi E. 2005. Evidence for the role of the oxygen-evolving manganese complex in photoinhibition of photosystem II. *Biochimica et Biophysica Acta* **1706**: 68–80.

Hakkila K, Antal T, Gunnelius L, Kurkela J, Matthijs HCP, Tyystjärvi E, Tyystjärvi T. 2013. Group 2 sigma factor mutant sigCDE of the cyanobacterium *Synechocystis* sp. PCC 6803 reveals functionality of both carotenoids and flavodiiron proteins in photoprotection of photosystem II. *Plant and Cell Physiology* **54**: 1780–1790.

Halliwell B, Gutteridge JMC. 2015. *Free radicals in biology and medicine.* Oxford, UK: Oxford University Press.

Han GY, Mamedov F, Styring S. 2012. Misses during water oxidation in photosystem II are S-state dependent. *Journal of Biological Chemistry* **287**: 13422–13429.

Havurinne V, Aitokari R, Mattila H, Käpylä V, Tyystjärvi E. 2021. Ultraviolet screening by slug tissue and tight packing of plastids protect photosynthetic sea slugs from photoinhibition. *Photosynthesis Research* **152**: 373–387.

Havurinne V, Tyystjärvi E. 2017. Action spectrum of photoinhibition in the diatom *Phaeodactylum tricornutum*. *Plant and Cell Physiology* **58**: 2217–2225.

Hideg É, Barta C, Kálai T, Vass I, Hideg K, Asada K. 2002. Detection of singlet oxygen and superoxide with fluorescent sensors in leaves under stress by photoinhibition or UV radiation. *Plant and Cell Physiology* **43**: 1154–1164.

Hideg É, Spetea C, Vass I. 1994. Singlet oxygen production in thylakoid membranes during photoinhibition as detected by EPR spectroscopy. *Photosynthesis Research* **39**: 191–199.

Hideg É, Vass I. 1996. UV-B induced free radical production in plant leaves and isolated thylakoid membranes. *Plant Science* **115**: 251–260.

Hillmann B, Brettel K, van Mieghem F, Kamlowski A, Rutherford WA, Schlodder E. 1995. Charge recombination reactions in photosystem II. 2. Transient absorbance difference spectra and their temperature dependence. *Biochemistry* **34**: 4814–4827.

Hoops S, Sahle S, Gauges R, Lee C, Pahle J, Simus N, Singhal M, Xu L, Mendes P, Kummer U. 2006. COPASI – a COmplex PAthway SImulator. *Bioinformatics* **22**: 3067–3074.

Horner O, Anxolabéhère-Mallart E, Charlot M-F, Tchertanov L, Guilhem J, Mattioloi TA, Boussac A, Girerd J-J. 1999. A new manganese dinuclear complex with phenolate ligands and a single unsupported oxo bridge. Storage of two positive charges within less than 500 mV. Relevance to photosynthesis. *Inorganic Chemistry* **38**: 1222–1232.

Isgandarova S, Renger G, Messinger J. 2003. Functional differences of photosystem II from *Synechococcus elongatus* and spinach characterized by flash induced oxygen evolution patterns. *Biochemistry* **42**: 8929–8938.

Jahns P, Depka B, Trebst A. 2000. Xanhophyll cycle mutants from *Chlamydomonas reinhardtii* indicate a role for zeaxanthin in the D1 protein turnover. *Plant Physiology and Biochemistry* **38**: 371–376.

Jegerschöld C, Styring S. 1996. Spectroscopic characterization of intermediate steps involved in donor-side-induced photoinhibition of photosystem II. *Biochemistry* **35**: 7794–7801.

Jones LW, Kok B. 1966. Photoinhibition of chloroplast reactions. I. Kinetics and action spectra. *Plant Physiology* **41**: 1037–1043.

Keren N, Berg A, Van Kan PJM, Levanon H, Ohad I. 1997. Mechanism of photosystem II photoinactivation and D1 protein degradation at low light: the role of back electron flow. *Proceedings of the National Academy of Sciences, USA* **94**: 1579–1584.

Kornyeyev D, Holaday S, Logan B. 2003. Predicting the extent of photosystem II photoinactivation using chlorophyll *a* fluorescence parameters measured during illumination. *Plant and Cell Physiology* **44**: 1064–1070.

Kramer DM, Johnson G, Kiirats O, Edwards GE. 2004. New flux parameters for the determination of Q_A redox state and excitation fluxes. *Photosynthesis Research* **79**: 209–218.

Lazarova D, Stanoeva D, Popova A, Vasilev D, Velitchkova M. 2014. UV-B induced alteration of oxygen evolving reactions in pea thylakoid membranes as affected by scavengers of reactive oxygen species. *Biologia Plantarum* **58**: 319–327.

Lee KP, Kim C, Landgraf F, Apel K. 2007. EXECUTER1- and EXECUTER2-dependent transfer of stress-related signals from the plastid to the nucleus of *Arabidopsis thaliana*. *Proceedings of the National Academy of Sciences, USA* **104**: 10270–10275.

Lendzian F, Bittl R, Telfer A, Lubitz W. 2003. Hyperfine structure of the photoexcited triplet state $^3P_{680}$ in plant PS II reaction centres as determined by pulse ENDOR spectroscopy. *Biochimica et Biophysica Acta* **1605**: 35–46.

Macpherson AN, Telfer A, Barber J, Truscott G. 1993. Direct detection of singlet oxygen from isolated photosystem II reaction centres. *Biochimica et Biophysica Acta* **1143**: 301–309.

Mao Z, Campbell CT. 2019. Apparent activation energies in complex reaction mechanisms: a simple relationship via degrees of rate control. *ACS Catalysis* **9**: 9465–9473.

Mattila H, Mishra KB, Kuusisto I, Mishra A, Novotna K, Šebela D, Tyystjärvi E. 2020. Effects of low temperature on photoinhibition and singlet oxygen production in four natural accessions of Arabidopsis. *Planta* **252**: 19.

Messinger J, Renger G. 1994. Analyses of pH-induced modifications of the period four oscillation of flash-induced oxygen evolution reveal distinct structural changes of the photosystem II donor side at characteristic pH values. *Biochemistry* **33**: 10896–10905.

Moser CC, Page CC, Dutton PL. 2005. Tunneling in PSII. *Photochemical and Photobiological Sciences* **4**: 933–939.

Nedbal L, Samson G, Whitmarsh J. 1992. Redox state of a one-electron component controls the rate of photoinhibition of photosystem II. *Proceedings of the National Academy of Sciences, USA* **89**: 7929–7933.

Nishiyama Y, Allakhverdiev SI, Yamamoto H, Hayashi H, Murata N. 2004. Singlet oxygen inhibits the repair of photosystem II by suppressing the translation elongation of the D1 protein in *Synechocystis* sp. PCC 6803. *Biochemistry* **43**: 11321–11330.

Ohnishi N, Allakhverdiev SI, Takahashi S, Higashi S, Watanabe M, Nishiyama Y, Murata N. 2005. Two-step mechanism of photodamage to photosystem II: step 1 occurs at the oxygen-evolving complex and step 2 occurs at the photochemical reaction center. *Biochemistry* **44**: 8494–8499.

Oxborough K, Baker NR. 1997. Resolving chlorophyll *a* fluorescence images of photosynthetic efficiency into photochemical and non-photochemical components – calculation of qP and Fv′/Fm′ without measuring Fo′. *Photosynthesis Research* **54**: 135–142.

Pham LV, Olmos JDJ, Chernev P, Kargul J, Messinger J. 2019. Unequal misses during the flash-induced advancement of photosystem II: effect of the S-state and acceptor side cycles. *Photosynthesis Research* **139**: 93–106.

Prasad A, Sedlarova M, Pospíšil P. 2018. Singlet oxygen imaging using fluorescent probe singlet oxygen sensor green in photosynthetic organisms. *Scientific Reports* **8**: 13685.

Ramel F, Birtic S, Cuiné S, Triantaphylidès C, Ravanat JL, Havaux M. 2012a. Chemical quenching of singlet oxygen by carotenoids in plants. *Plant Physiology* **158**: 1267–1278.

Ramel F, Birtic S, Ginies C, Soubigou-Taconnat L, Triantaphylidès C, Havaux M. 2012b. Carotenoid oxidation products are stress signals that mediate gene responses to singlet oxygen in plants. *Proceedings of the National Academy of Sciences, USA* **109**: 5535–5540.

Randall JT, Wilkins MHF. 1945. Phosphorescence and electron traps. I. The study of trap distribution. *Proceedings of the Royal Society A* **184**: 366–389.

Rantamäki S, Tyystjärvi E. 2011. Analysis of the S2QA- charge recombination with the Arrhenius, Eyring and Marcus theories. *Journal of Photochemistry and Photobiology B* **104**: 292–300.

Rappaport F, Lavergne J. 2009. Thermoluminescence: theory. *Photosynthesis Research* **101**: 205–216.

Rehman AU, Cser K, Sass L, Vass I. 2013. Characterization of singlet oxygen production and its involvement in photodamage of photosystem II in the cyanobacterium *Synechocystis* PCC 6803 by histidine-mediated chemical trapping. *Biochimica et Biophysica Acta* **1827**: 689–698.

Renger G, Wolff CH. 1976. The existence of a high photochemical turnover rate at the reaction centers of system II in tris-washed chloroplasts. *Biochimica et Biophysica Acta* **4233**: 610–614.

Rippka R, Deruelles J, Waterbury JB, Herdman M, Stanier RY. 1979. Generic assignments, strain histories and properties of pure cultures of cyanobacteria. *Journal of General Microbiology* **111**: 1–61.

Rutherford AW. 1989. Photosystem II, the water-splitting enzyme. *Trends in Biochemical Sciences* **14**: 227–232.

Santabarbara S, Agostini G, Casazza AP, Syme CD, Heathcote P, Böhles F, Evans MCW, Jennngs RC, Carbonera D. 2007. Chlorophyll triplet states associated with photosystem I and photosystem II in thylakoids of the green alga *Chlamydomonas reinhardtii*. *Biochimica et Biophysica Acta* **1767**: 88–105.

Santabarbara S, Bordignon E, Jennings RC, Carbonera D. 2002. Chlorophyll triplet states associated with photosystem II of thylakoids. *Biochemistry* **41**: 8184–8194.

Santabarbara S, Jennings RC, Carbonera D. 2003. Analysis of photosystem II triplet states in thylakoids by fluorescence detected magnetic resonance in relation to the redox state of the primary quinone acceptor Q_A. *Chemical Physics* **294**: 257–266.

Santabarbara S, Neverov KV, Garlaschi FM, Zucchelli RC. 2001. Involvement of uncoupled antenna chlorophylls in photoinhibition in thylakoids. *FEBS Letters* **491**: 109–113.

Sarvikas P, Hakala M, Pätsikkä E, Tyystjärvi T, Tyystjärvi E. 2006. Action spectrum of photoinhibition in leaves of wild type and npq1-2 and npq4-1 mutants of *Arabidopsis thaliana*. *Plant and Cell Physiology* **47**: 391–400.

Schweitzer C, Schmidt R. 2003. Physical mechanisms of generation and deactivation of singlet oxygen. *Chemical Reviews* **103**: 1685–1757.

Sipka G, Magyar M, Mezzetti A, Akhtar P, Zhu Q, Xiao Y, Han G, Santabarbara S, Shen J-R, Lambrev P *et al.* 2021. Light-adapted charge-separated state of photosystem II: structural and functional dynamics of the closed reaction center. *Plant Cell* **33**: 1286–1302.

Sundby C, Mattsson M, Schiött T. 1992. Effects of bicarbonate and oxygen concentration on photoinhibition of thylakoid membranes. *Photosynthesis Research* **34**: 263–270.

Telfer A, Bishop SM, Phillips D, Barber J. 1994. Isolated photosynthetic reaction center of photosystem II as a sensitizer for the formation of singlet oxygen. Detection and quantum yield determination using a chemical trapping technique. *Journal of Biological Chemistry* **269**: 13244–13253.

Treves H, Raanan H, Kedem I, Murik O, Keren N, Zer H, Berkowicz SM, Giordano M, Norici A, Shotland Y *et al.* 2016. The mechanisms whereby the green alga *Chlorella ohadii*, isolated from desert soil crust, exhibits unparalleled photodamage resistance. *New Phytologist* **210**: 1229–1243.

Tsonev TD, Hikosaka K. 2003. Contribution of photosynthetic electron transport, heat dissipation, and recovery of photoinactivated photosystem II to photoprotection at different temperatures in *Chenopodium album* leaves. *Plant and Cell Physiology* **44**: 828–835.

Tyystjärvi E. 2013. Photoinhibition of photosystem II. *International Review of Cell and Molecular Biology* **300**: 243–303.

Tyystjärvi E, Aro EM. 1996. The rate constant of photoinhibition, measured in lincomycin-treated leaves, is directly proportional to light intensity. *Proceedings of the National Academy of Sciences, USA* **93**: 2213–2218.

Tyystjärvi E, Kettunen R, Aro E-M. 1994. The rate constant of photoinhibition *in vitro* is independent of the antenna size of photosystem II but depends on temperature. *Biochimica et Biophysica Acta* **1186**: 177–185.

Tyystjärvi E, Rantamäki S, Tyystjärvi J. 2009. Connectivity of photosystem II is the physical basis of retrapping in photosynthetic thermoluminescence. *Biophysical Journal* **96**: 3735–3743.

Tyystjärvi E, Vass I. 2004. Light emission as a probe of charge separation and recombination in the photosynthetic apparatus. Relation of prompt fluorescence to delayed light emission and thermoluminescence. In: Papageorgiou GC, Govindjee, eds. *Chlorophyll* a *fluorescence. A signature of photosynthesis. Advances in photosynthesis and respiration, vol. 19*. Dordrecht, the Netherlands: Kluwer Academic, 363–388.

Ueno M, Sae-Tang P, Kusama Y, Hihara Y, Matsuda M, Hasunuma T, Nishiyama Y. 2016. Moderate heat stress stimulates repair of photosystem II during photoinhibition in *Synechocystis* sp. PCC 6803. *Plant and Cell Physiology* **57**: 2417–2426.

Vass I. 2011. Role of charge recombination processes in photodamage and photoprotection of the photosystem II complex. *Physiologia Plantarum* **142**: 6–16.

Vass I. 2012. Molecular mechanisms of photodamage in the photosystem II complex. *Biochimica et Biophysica Acta* **1817**: 209–217.

Vass I, Govindjee. 1996. Thermoluminescence from the photosynthetic apparatus. *Photosynthesis Research* **48**: 117–126.

Vass I, Styring S. 1993. Characterization of chlorophyll triplet promoting states in photosystem II sequentially induced during photoinhibition. *Biochemistry* **32**: 3334–3341.

Zabelin AA, Neverov KV, Krasnovsky AA, Shkuropatova VA, Shuvalov VA, Shkuropatov AY. 2016. Characterization of the low-temperature triplet state of chlorophyll in photosystem II core complexes: application of phosphorescence measurements and Fourier transform infrared spectroscopy. *Biochimica et Biophysica Acta – Bioenergetics* **1857**: 782–788.

Zavafer A, Mancilla C. 2021. Concepts of photochemical damage of photosystem II and the role of excessive excitation. *Journal of Photochemistry and Photobiology C Photochemistry Reviews* **47**: 100421.

Supporting Information

Additional Supporting Information may be found online in the Supporting Information section at the end of the article.

Fig. S1 Energy spectra of light sources used in the present study.

Fig. S2 Temperature dependence of the histidine method.

Fig. S3 Effect of temperature on the yield of photosystem II electron transfer.

Fig. S4 Measurements of photoinhibition of photosystem II.

Fig. S5 Photoinhibition under anaerobic conditions, in the absence or presence of sodium bicarbonate.

Fig. S6 Temperature dependences of dark inactivation in the absence and presence of histidine or in the absence and presence of α-tocopherol.

Fig. S7 Detection of carbon-centered radicals from pumpkin thylakoids with α-(4-pyridyl 1-oxide)-*N*-*tert*-butylnitrone.

Fig. S8 pH dependence of photoinhibition.

Fig. S9 Comparison of fluorescence and oxygen evolution assays for quantification of photoinhibition.

Methods S1 Calculations.

Table S1 Parameters obtained from the thermoluminescence measurements.

Please note: Wiley is not responsible for the content or functionality of any Supporting Information supplied by the authors. Any queries (other than missing material) should be directed to the *New Phytologist* Central Office.